

SUPERCONVERGENCE ANALYSIS OF LINEAR FEM BASED ON THE POLYNOMIAL PRESERVING RECOVERY AND RICHARDSON EXTRAPOLATION FOR HELMHOLTZ EQUATION WITH HIGH WAVE NUMBER

YU DU**, HAIJUN WU^{††}, AND ZHIMIN ZHANG^{‡‡}

Abstract. We study superconvergence property of the linear finite element method with the polynomial preserving recovery (PPR) and Richardson extrapolation for the two dimensional Helmholtz equation. The H^1 -error estimate with explicit dependence on the wave number k is derived. First, we prove that under the assumption $k(kh)^2 \leq C_0$ (h is the mesh size) and certain mesh condition, the estimate between the finite element solution and the linear interpolation of the exact solution is superconvergent under the H^1 -seminorm, although the pollution error still exists. Second, we prove a similar result for the recovered gradient by PPR and found that the PPR can only improve the interpolation error and has no effect on the pollution error. Furthermore, we estimate the error between the finite element gradient and recovered gradient and discovered that the pollution error is canceled between these two quantities. Finally, we apply the Richardson extrapolation to recovered gradient and demonstrate numerically that PPR combined with the Richardson extrapolation can reduce the interpolation and pollution errors simultaneously, and therefore, leads to an asymptotically exact *a posteriori* error estimator. All theoretical findings are verified by numerical tests.

Key words. Helmholtz equation, large wave number, pollution errors, superconvergence, polynomial preserving recovery, finite element methods

AMS subject classifications. 65N12, 65N15, 65N30, 78A40

1. Introduction. Let $\Omega \in \mathbb{R}^2$ be a bounded polygon with boundary $\Gamma := \partial\Omega$. We consider the Helmholtz problem:

$$(1.1) \quad -\Delta u - k^2 u = f \quad \text{in } \Omega,$$

$$(1.2) \quad \frac{\partial u}{\partial n} + \mathbf{i}ku = g \quad \text{on } \Gamma,$$

where $\mathbf{i} = \sqrt{-1}$ denotes the imaginary unit and n denotes the unit outward normal to Γ . The above Helmholtz problem is an approximation of the following acoustic scattering problem (with time dependence $e^{\mathbf{i}\omega t}$):

$$(1.3) \quad -\Delta u - k^2 u = f \quad \text{in } \mathbb{R}^2,$$

$$(1.4) \quad \sqrt{r} \left(\frac{\partial(u - u^{inc})}{\partial r} + \mathbf{i}k(u - u^{inc}) \right) \rightarrow 0 \quad \text{as } r = |x| \rightarrow \infty,$$

*Beijing computational science research center, Beijing, 100193, China. duyu87@csrc.ac.cn, dynju@qq.com. This research work is supported by a Tianhe-2JK computing time award at the Beijing Computational Science Research Center (CSRC). The research of this author was supported in part by the China Postdoctoral Science Foundation under grant 2016M591053 and the National Natural Science Foundation of China under grants 11601026

^{††}Department of Mathematics, Nanjing University, Jiangsu, 210093, China. hjw@nju.edu.cn. This research was partially supported by the National Natural Science Foundation of China under grants 11525103 and 91130004.

^{‡‡}Beijing Computational Science Research Center, Beijing, 100193 and Department of Mathematics, Wayne State University, Detroit, MI 48202. zmzhang@csrc.ac.cn, zzhang@math.wayne.edu. The research of this author was supported in part by the National Natural Science Foundation of China under grants 11471031, 91430216, U1530401, and the U.S. National Science Foundation through grant DMS-1419040.

where u^{inc} is the incident wave and k is known as the wave number. The Robin boundary condition (1.2) is known as the first order approximation of the radiation condition (1.4) (cf. [17]). We remark that the Helmholtz problem (1.1)–(1.2) also arises in applications as a consequence of frequency domain treatment of attenuated scalar waves (cf. [14]).

We know that the finite element method of fixed order for the Helmholtz problem (1.1)–(1.2) at high frequencies ($k \gg 1$) is subject to the effect of pollution: the ratio of the error of the finite element solution to the error of the best approximation from the finite element space cannot be uniformly bounded with respect to k [2, 5, 4, 13, 20, 22, 23]. More precisely, the linear finite element method for a 2-D Helmholtz problem satisfies the following error estimate under the mesh constraint $k(kh)^2 \leq C_0$ [42, 15]:

$$(1.5) \quad \|\nabla(u - u_h)\|_{L^2(\Omega)} \leq C_1 kh + C_2 k(kh)^2.$$

Here u_h is the linear finite element solution, h is the mesh size and $C_i, i = 1, 2$ are positive constants independent of k and h . It is easy to see that the order of the first term on the right hand side of (1.5) is the same to that of the interpolation error in H^1 -seminorm and it can dominate the error bound only if $k(kh)$ is small enough. However, the second term on the right-hand side of (1.5) dominates the estimate under other mesh conditions. For example, kh is fixed and k is large enough. The term $C_2 k(kh)^2$ is called the pollution error of the finite element solution.

Considerable efforts have been made in analysis of different numerical methods for the Helmholtz problem with large wave number in the literature. The readers are referred to [3, 14, 31] for asymptotic error estimates of general DG methods and [22, 23] for pre-asymptotic error estimates of a one-dimensional problem discretized on equidistant grid. For more pre-asymptotic error estimates, Please refer to [28, 29] and [9, 42] for classical finite element methods as well as interior penalty finite element methods. For other methods solving the Helmholtz problems, such as the interior penalty discontinuous Galerkin method or the source transfer domain decomposition method, one can read [27, 18, 19, 41, 16, 11].

In this work, we investigate the superconvergence property of the linear finite element method when being post-processed by the polynomial preserving recovery (PPR) for the Helmholtz problem. PPR was proposed by Zhang and Naga [40] in 2004 and has been successfully applied to finite element methods. COMSOL Multiphysics adopted PPR as a post-processing tool since 2008 [1]. One important feature of PPR is its superconvergence property for the recovered gradient. To learn more about PPR, readers are referred to [38, 37, 30, 34]. Some theoretical results about recovery techniques and recovery-type error estimators can be found in [6, 24, 39, 35, 36].

Let V_h be the linear finite element space and denote $G_h : V_h \rightarrow V_h \times V_h$ as the gradient recovery operator from PPR. We obtain the following estimate:

$$(1.6) \quad \|\nabla u - G_h u_h\|_{L^2(\Omega)} \lesssim kh^{1+\alpha} + k(kh)^2, \quad (0 < \alpha \leq 1)$$

under the mesh condition $k(kh)^2 \leq C$, where C is a constant independent of k and h . Furthermore, we prove

$$\|G_h u_h - \nabla u_h\|_{L^2(\Omega)} \lesssim kh + k(kh)^3,$$

which means that $\|G_h u_h - \nabla u_h\|_{L^2(\Omega)}$, i.e., using PPR alone, can not measure the H^1 -error of the numerical solution well. However, the super-convergence $O(h^2)$ of the recovered gradient with $\alpha = 1$ makes it possible to apply the Richardson extrapolation

on the recovered gradient of the numerical solution. We show the asymptotic exactness of the a posteriori error estimator $\|RG_h u_h - \nabla u_h\|_{L^2(\Omega)}$ by numerical tests, where R is the Richardson extrapolation operator.

The remainder of this paper is organized as follows: some notations, FEM and the mesh constraints are introduced in section 2. In section 3, we prove the superconvergence between the interpolant and the finite element solution to the problem with Robin boundary (1.1)–(1.2). In section 4, we prove the superconvergence property of G_h in the Sobolev space H^3 and show the most important result, that is the error estimate of $G_h u_h$. Then we try to give the reason for the effect of G_h to the pollution error in section 5. Finally, we simulate a model problem by the linear FEM, PPR method and the Richardson extrapolation in section 6. It is shown that the recovered gradient can be improved by the Richardson extrapolation further and the a posterior error estimator based on the PPR and Richardson extrapolation is exact asymptotically.

Throughout the paper, C is used to denote a generic positive constant which is independent of h, k, f and g . We also use the shorthand notation $A \lesssim B$ and $A \gtrsim B$ for the inequality $A \leq CB$ and $A \geq B$. $A \approx B$ is a shorthand notation for the statement $A \lesssim B$ and $B \lesssim A$. We assume that $k \gg 1$ since we are considering high-frequency problems and that k is constant on Ω for ease of presentation. We also assume that Ω is a strictly star-shaped domain. Here “strictly star-shaped” means that there exist a point $x_\Omega \in \Omega$ and a positive constant c_Ω depending only on Ω such that

$$(x - x_\Omega) \cdot n \geq c_\Omega \quad \forall x \in \Gamma.$$

2. Preliminaries. We first introduce some notation. The standard Sobolev and Hilbert space, norm, and inner product notation are adopted. Their definitions can be found in [8, 12]. In particular, $(\cdot, \cdot)_Q$ and $\langle \cdot, \cdot \rangle_\Sigma$ for $\Sigma = \partial Q$ denote the L^2 -inner product on complex-valued $L^2(Q)$ and $L^2(\Sigma)$ spaces, respectively. For simplicity, we denote $(\cdot, \cdot) := (\cdot, \cdot)_\Omega$, $\langle \cdot, \cdot \rangle := \langle \cdot, \cdot \rangle_{\partial\Omega}$, $\|\cdot\|_j := \|\cdot\|_{H^j(\Omega)}$, and $|\cdot|_j := |\cdot|_{H^j(\Omega)}$.

Let \mathcal{T}_h be a regular triangulation of the domain Ω , \mathcal{E}_h be the set of all edges of \mathcal{T}_h and \mathcal{N}_h be the set of all nodal points. For any $\tau \in \mathcal{T}_h$, we denote by h_τ its diameter and by $|\tau|$ its area. Similarly, for each edge $e \in \mathcal{E}_h$, define $h_e := \text{diam}(e)$. Let $h = \max_{\tau \in \mathcal{T}_h} h_\tau$. Assume that $h_\tau \approx h$. We denote all the boundary edges by $\mathcal{E}_h^B := \{e \in \mathcal{E}_h : e \subset \Gamma\}$ and the interior edges by $\mathcal{E}_h^I := \mathcal{E}_h \setminus \mathcal{E}_h^B$.

Let V_h be the approximation space of continuous piecewise linear polynomials, that is,

$$V_h := \{v_h \in H^1(\Omega) : v_h|_\tau \in P_1(\tau) \quad \forall \tau \in \mathcal{T}_h\},$$

where $P_1(\tau)$ denotes the set of all polynomials defined on τ with degree ≤ 1 .

Denote by $a(u, v) = (\nabla u, \nabla v) \quad \forall u, v \in H^1(\Omega)$. The variational problem to (1.1)–(1.2) reads as follows: Find $u \in H^1(\Omega)$ such that

$$(2.1) \quad a(u, v) - k^2(u, v) + \mathbf{i}k \langle u, v \rangle = (f, v) + \langle g, v \rangle \quad \forall v \in H^1(\Omega).$$

Then the linear finite element solution $u_h \in V_h$ satisfies

$$(2.2) \quad a(u_h, v_h) - k^2(u_h, v_h) + \mathbf{i}k \langle u_h, v_h \rangle = (f, v_h) + \langle g, v_h \rangle \quad \forall v_h \in V_h.$$

Throughout the paper, we assume that the data f is sufficiently smooth and $g \in H^2(\Gamma)$ such that $u \in H^3(\Omega)$. Denote by

$$(2.3) \quad C_{u,g} = \sum_{j=1}^3 k^{-(j-1)} \|u\|_j + \sum_{j=1}^2 k^{-j} |g|_{H^j(\Gamma)}.$$

We remark that in recent years there have been some superconvergence results for recovered gradients [34, 35, 36]. All of them assumed at least $u \in H^3(\Omega) \cap W_\infty^2(\Omega)$ instead of $u \in H^3(\Omega)$. The function $C_{u,g}$ could be treated as a constant in this paper since $\|u\|_j$ is bounded by $\max(k^0, k^{j-1})$. The reader is referred to [27, 28, 29] for the estimates of u .

The following norm on $H^1(\Omega)$ is useful for the subsequent analysis:

$$(2.4) \quad \|v\| := (\|\nabla v\|_0^2 + k^2 \|v\|_0^2)^{\frac{1}{2}} \quad \forall v \in H^1(\Omega).$$

The following lemma is proved in [42, 15].

LEMMA 2.1. *For u and u_h , the solutions to (1.1)–(1.2) and (2.2), there exists a constant C_0 independent of k and h such that if $k(kh)^2 \leq C_0$, then the following error estimates hold:*

$$\begin{aligned} \|u - u_h\|_1 &\lesssim (kh + k(kh)^2) \frac{|u|_2}{k}, \\ k \|u - u_h\|_0 &\lesssim ((kh)^2 + k(kh)^2) \frac{|u|_2}{k}. \end{aligned}$$

Note that $k^{-1}|u|_2 \leq C_{u,g}$.

We begin with some definitions regarding meshes. For an interior edge $e \in \mathcal{E}_h^I$, we denote $\Omega_e = \tau_e \cup \tau'_e$, a patch formed by the two elements τ_e and τ'_e sharing e , see Figures 2.1–2.2. For any edge $e \in \mathcal{E}_h$ and an element τ with $e \subset \tau$, θ_e denotes the angle opposite of the edge e in τ , \mathbf{t}_e denotes the unit tangent vector of e with counterclockwise orientation and \mathbf{n}_e , the unit outward normal vector of e , h_e, h_{e+1} , and h_{e-1} denote the lengths of the three edges of τ , respectively. Here the subscript $e+1$ or $e-1$ is for orientation. Note that all triangles in the triangulation are orientated counterclockwise, and the index $'$ is added for the corresponding quantities in τ' with $\mathbf{t}_e = -\mathbf{t}'_e$ and $\mathbf{n}_e = -\mathbf{n}'_e$ due to the orientation.

For any $e \in \mathcal{E}_h^I$ (cf. Figure 2.1), we say that Ω_e is an ε approximate parallelogram if the lengths of any two opposite edges differ by at most ε , that is,

$$|h_{e-1} - h'_{e-1}| + |h_{e+1} - h'_{e+1}| \leq \varepsilon.$$

For any $e \in \mathcal{E}_h^B$ (cf. Figure 2.2), we say that τ_e is an ε approximate isosceles triangle if the lengths of its two edges $e-1$ and $e+1$ differ by at most ε , that is,

$$|h_{e+1} - h_{e-1}| \leq \varepsilon.$$

DEFINITION 2.2. *The triangulation \mathcal{T}_h is said to satisfy α approximation condition if there exists a constant $\alpha \geq 0$ such that*

- (a) *the patch Ω_e is an $O(h^{1+\alpha})$ approximate parallelogram for any interior edge $e \in \mathcal{E}_h^I$;*
- (b) *the triangle τ_e is an $O(h^{1+\alpha})$ approximate isosceles triangle for any boundary edge $e \in \mathcal{E}_h^B$;*

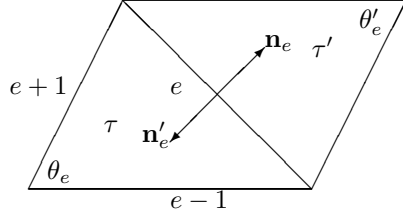
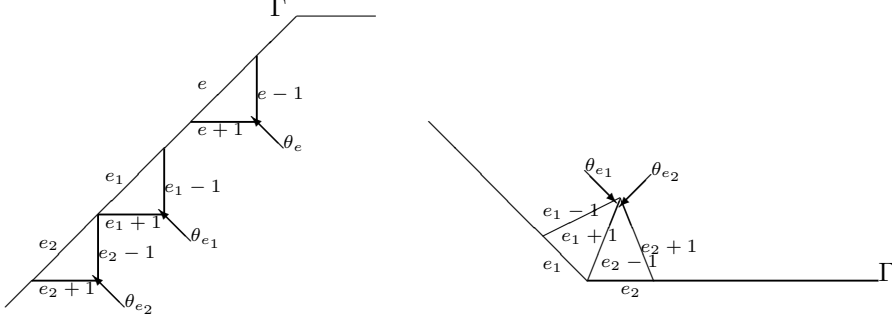
FIG. 2.1. Notation in the patch Ω_e .

FIG. 2.2. Notation in the boundary elements.

Remark 2.1. For interior edges, the restriction “ $h^{1+\alpha}$ approximate parallelogram” is often used to prove the superconvergence property for problems with the Dirichlet boundary condition [10, 34], when boundary edges \mathcal{E}_h^B can be ignored since $u_h - u_I \equiv 0$ where u_I is the linear interpolant of u . However, ignoring the edges in \mathcal{E}_h^B is impossible for the Robin condition (1.2). As a result, more restrictions are put on the boundary edges. Note that this restriction is technique and just for theoretical purpose. In fact, one can still get results of superconvergence under general meshes which do not satisfy the condition, such as Chevron pattern uniform mesh.

3. Superconvergence between the finite element solution and linear interpolant. Different from most other investigations in the literatures where the Dirichlet boundary condition is assumed, we consider the superconvergence between the FE solution u_h under the Robin boundary condition and the linear interpolant u_I of the exact solution u . Since u_h may not equal u_I on the boundary Γ , some more strict mesh conditions and special arguments are needed to establish the desired superconvergence result.

First we introduce a quadratic interpolant $\psi_Q = \Pi_Q \psi$ of ψ based on nodal values and moment conditions on edges,

$$(3.1) \quad (\Pi_Q \phi)(z) = \phi(z), \quad \int_e \Pi_Q \phi = \int_e \phi \quad \forall z \in \mathcal{N}_h, e \in \mathcal{E}_h.$$

The following fundamental identity for $v_h \in P_1(\tau)$ has been proved in [10]:

$$(3.2) \quad \int_\tau \nabla(\phi - \phi_I) \cdot \nabla v_h = \sum_{e \in \partial\tau} \left(\beta_e \int_e \frac{\partial^2 \phi_Q}{\partial \mathbf{t}_e^2} \frac{\partial v_h}{\partial \mathbf{t}_e} + \gamma_e \int_e \frac{\partial^2 \phi_Q}{\partial \mathbf{t}_e \partial \mathbf{n}_e} \frac{\partial v_h}{\partial \mathbf{t}_e} \right)$$

where

$$(3.3) \quad \beta_e = \frac{1}{12} \cot \theta_e (h_{e+1}^2 - h_{e-1}^2), \quad \gamma_e = \frac{1}{3} \cot \theta_e |\tau|,$$

and $\phi_I \in P_1(\tau)$ is the linear interpolant of ϕ on τ . The following lemma can be easily obtained [10, 34].

LEMMA 3.1. *We denote \mathbf{m}_e by \mathbf{t}_e or \mathbf{n}_e . Assume that \mathcal{T}_h satisfies the α approximation condition, then we have the following estimates:*

(a) *For any interior edge $e \in \mathcal{E}_h^I$,*

$$(3.4) \quad |\beta_e| + |\beta'_e| \lesssim h^2, \quad |\gamma_e| + |\gamma'_e| \lesssim h^2;$$

$$(3.5) \quad |\beta_e - \beta'_e| \lesssim h^{2+\alpha}, \quad |\gamma_e - \gamma'_e| \lesssim h^{2+\alpha}.$$

(b) *For two adjacent edges $e_1, e_2 \in \mathcal{E}_h^B$, that is $e_1 \cap e_2 \neq \emptyset$,*

$$(3.6) \quad |\beta_{e_1}| + |\beta_{e_2}| \lesssim h^{2+\alpha}, \quad |\gamma_{e_1}| + |\gamma_{e_2}| \lesssim h^2$$

$$(3.7) \quad |\gamma_{e_1} - \gamma_{e_2}| \lesssim h^{2+\alpha}$$

(c) *For any edge $e \in \mathcal{E}_h$, $e \subset \partial\tau_e$,*

$$(3.8) \quad \int_e \frac{\partial^2 \phi}{\partial \mathbf{t}_e \partial \mathbf{m}_e} \frac{\partial v_h}{\partial \mathbf{t}_e} \lesssim (\|\phi\|_{H^3(\tau_e)} + h^{-1} \|\phi\|_{H^2(\tau_e)}) \|\nabla v_h\|_{L^2(\tau_e)};$$

$$(3.9) \quad \int_e \frac{\partial^2(\phi - \phi_Q)}{\partial \mathbf{t}_e \partial \mathbf{m}_e} \frac{\partial v_h}{\partial \mathbf{t}_e} \lesssim |\phi|_{H^3(\tau_e)} \|\nabla v_h\|_{L^2(\tau_e)}.$$

Proof. The inequalities (3.4)–(3.6) follow from the α approximation condition. From the condition (a) and (b) in Definition 2.2, we have for any $e_1, e_2 \in \mathcal{E}_h^B$ satisfying $e_1 \cap e_2 \neq \emptyset$ (cf. Figure 2.2),

$$\frac{|h_{e_1-1} h_{e_1+1} \cos \theta_{e_1} - h_{e_2-1} h_{e_2+1} \cos \theta_{e_2}|}{h} \lesssim h^{1+\alpha},$$

which implies (3.7).

Finally, the inequalities (3.8) and (3.9) follow from the trace theorem. \square

LEMMA 3.2. *Assume that \mathcal{T}_h satisfies the α approximation condition. Then for any $v_h \in V_h$,*

$$(3.10) \quad \left| \int_{\Omega} \nabla(u - u_I) \cdot \nabla v_h \right| \lesssim ((kh)^2 + kh^{1+\alpha}) \|\nabla v_h\|_{L^2(\Omega)} C_{u,g}.$$

Here u_I is the linear interpolant of u on Ω .

Proof. From (3.2), we have

$$\begin{aligned} \int_{\Omega} \nabla(u - u_I) \cdot \nabla v_h &= \sum_{\tau \in \mathcal{T}_h} \sum_{e \subset \partial\tau} \left(\beta_e \int_e \frac{\partial^2 u_Q}{\partial \mathbf{t}_e^2} \frac{\partial v_h}{\partial \mathbf{t}_e} + \gamma_e \int_e \frac{\partial^2 u_Q}{\partial \mathbf{t}_e \partial \mathbf{n}_e} \frac{\partial v_h}{\partial \mathbf{t}_e} \right) \\ &= I_1 + I_2, \end{aligned}$$

where

$$\begin{aligned}
I_1 &= \sum_{e \in \mathcal{E}_h^I} \left[(\beta_e - \beta'_e) \int_e \frac{\partial^2 u}{\partial t_e^2} \frac{\partial v_h}{\partial t_e} + (\gamma_e - \gamma'_e) \int_e \frac{\partial^2 u}{\partial t_e \partial n_e} \frac{\partial v_h}{\partial t_e} \right. \\
&\quad + \beta_e \int_e \frac{\partial^2 (u_Q - u)}{\partial t_e^2} \frac{\partial v_h}{\partial t_e} + \gamma_e \int_e \frac{\partial^2 (u_Q - u)}{\partial t_e \partial n_e} \frac{\partial v_h}{\partial t_e} \\
&\quad \left. + \beta'_e \int_e \frac{\partial^2 (u - u_Q)}{\partial t_e^2} \frac{\partial v_h}{\partial t_e} + \gamma'_e \int_e \frac{\partial^2 (u - u_Q)}{\partial t_e \partial n_e} \frac{\partial v_h}{\partial t_e} \right], \\
I_2 &= \sum_{e \in \mathcal{E}_h^B} \left[\beta_e \int_e \frac{\partial^2 u}{\partial t_e^2} \frac{\partial v_h}{\partial t_e} + \gamma_e \int_e \frac{\partial^2 u}{\partial t_e \partial n_e} \frac{\partial v_h}{\partial t_e} \right. \\
&\quad \left. + \beta_e \int_e \frac{\partial^2 (u_Q - u)}{\partial t_e^2} \frac{\partial v_h}{\partial t_e} + \gamma_e \int_e \frac{\partial^2 (u_Q - u)}{\partial t_e \partial n_e} \frac{\partial v_h}{\partial t_e} \right].
\end{aligned}$$

First, I_1 can be estimated by Lemma 3.1 and Hölder's inequality:

$$\begin{aligned}
(3.11) \quad |I_1| &\lesssim \sum_{e \in \mathcal{E}_h^I} \left((h^{2+\alpha} + h^2) \|u\|_{H^3(\tau_e)} + h^{1+\alpha} \|u\|_{H^2(\tau_e)} \right) \|\nabla v_h\|_{L^2(\tau_e)} \\
&\lesssim ((h^{2+\alpha} + h^2) \|u\|_3 + h^{1+\alpha} \|u\|_2) \|\nabla v_h\|_0 \\
&\lesssim ((kh)^2 + kh^{1+\alpha}) \|\nabla v_h\|_0 C_{u,g}.
\end{aligned}$$

Next we estimate I_2 . From (3.6) and (3.9),

$$\begin{aligned}
(3.12) \quad I_{2,1} &:= \sum_{e \in \mathcal{E}_h^B} \left[\beta_e \int_e \frac{\partial^2 u}{\partial t_e^2} \frac{\partial v_h}{\partial t_e} + \beta_e \int_e \frac{\partial^2 (u_Q - u)}{\partial t_e^2} \frac{\partial v_h}{\partial t_e} + \gamma_e \int_e \frac{\partial^2 (u_Q - u)}{\partial t_e \partial n_e} \frac{\partial v_h}{\partial t_e} \right] \\
&\lesssim \sum_{e \in \mathcal{E}_h^B} (h^{1+\alpha} \|u\|_{H^2(\tau_e)} + (h^{2+\alpha} + h^2) \|u\|_{H^3(\tau_e)}) \|\nabla v_h\|_{L^2(\tau_e)} \\
&\lesssim (kh^{1+\alpha} + (kh)^2) \|\nabla v_h\|_0 C_{u,g}.
\end{aligned}$$

We turn to the estimate of the remaining terms of I_2 . Denote by z_i the nodes on Γ . Let e_1 and e_2 be two boundary edges in \mathcal{E}_h^B sharing z_i with counterclockwise orientation (cf. Figure 2.2). Denote by $[\gamma_e]_{z_i} = \gamma_{e_2} - \gamma_{e_1}$ and by \mathcal{N}_h^v the set of vertices of the domain Ω . Then we have

$$\begin{aligned}
(3.13) \quad \sum_{e \in \mathcal{E}_h^B} \gamma_e \int_e \frac{\partial^2 u}{\partial t_e \partial n_e} \frac{\partial v_h}{\partial t_e} &= - \sum_{e \in \mathcal{E}_h^B} \gamma_e \int_e \frac{\partial^3 u}{\partial t_e^2 \partial n_e} v_h + \sum_{z_i \in \Gamma \cap \mathcal{N}_h \setminus \mathcal{N}_h^v} [\gamma_e]_{z_i} \frac{\partial^2 u}{\partial t_e \partial n_e}(z_i) v_h(z_i) \\
&\quad + \sum_{z_i \in \mathcal{N}_h^v} \left(\gamma_{e_2} \frac{\partial^2 u}{\partial t_{e_2} \partial n_{e_2}}(z_i) v_h(z_i) - \gamma_{e_1} \frac{\partial^2 u}{\partial t_{e_1} \partial n_{e_1}}(z_i) v_h(z_i) \right) \\
&:= I_{2,2} + I_{2,3} + I_{2,4}.
\end{aligned}$$

It is easy to get

$$\begin{aligned}
(3.14) \quad I_{2,2} &= \sum_{e \in \mathcal{E}_h^B} \gamma_e \int_e \frac{\partial^3 u}{\partial t_e^2 \partial n_e} v_h \lesssim h^2 \left| \frac{\partial u}{\partial n} \right|_{H^2(\Gamma)} \|v_h\|_{L^2(\Gamma)} \\
&\lesssim h^2 (|g|_{H^2(\Gamma)} + k |u|_{H^2(\Gamma)}) \cdot \|v_h\|_0^{1/2} \|v_h\|_1^{1/2} \\
&\lesssim k^{3/2} h^2 \|v_h\| C_{u,g}.
\end{aligned}$$

Suppose that $w \in H^1([a, b])$ and denote by $h_{ab} = b - a$, we have

$$\begin{aligned} w^2(b) &= \int_a^b \left(\frac{x-a}{b-a} w^2(x) \right)' dx = \frac{1}{b-a} \int_a^b w^2 + 2 \int_a^b \frac{x-a}{b-a} w w' \\ &\leq \frac{1}{h_{ab}} \|w\|_{L^2([a,b])}^2 + 2 \|w\|_{H^1([a,b])} \|w\|_{L^2([a,b])}, \end{aligned}$$

which implies

(3.15)

$$\begin{aligned} I_{2,3} &\leq \sum_{z_i \in \Gamma \cap \mathcal{N}_h} |[\gamma_e]_{z_i}| \left(\frac{1}{h_{e_i}} \left| \frac{\partial u}{\partial n_{e_i}} \right|_{H^1(e_i)}^2 + 2 \left| \frac{\partial u}{\partial n_{e_i}} \right|_{H^2(e_i)} \left| \frac{\partial u}{\partial n_{e_i}} \right|_{H^1(e_i)} \right)^{1/2} \\ &\quad \cdot \left(\frac{1}{h_{e_i}} \|v_h\|_{L^2(e_i)}^2 + 2 \|v_h\|_{H^1(e_i)} \|v_h\|_{L^2(e_i)} \right)^{1/2} \\ &\lesssim \max_{z_i \in \Gamma \cap \mathcal{N}_h} |[\gamma_e]_{z_i}| \left(\frac{1}{h} \left| \frac{\partial u}{\partial n} \right|_{H^1(\Gamma)}^2 + \left| \frac{\partial u}{\partial n} \right|_{H^2(\Gamma)} \left| \frac{\partial u}{\partial n} \right|_{H^1(\Gamma)} \right)^{1/2} \\ &\quad \cdot \left(\frac{1}{h} \|v_h\|_{L^2(\Gamma)}^2 + \|v_h\|_{H^1(\Gamma)} \|v_h\|_{L^2(\Gamma)} \right)^{1/2} \\ &\lesssim \frac{\max_{z_i \in \Gamma \cap \mathcal{N}_h} |[\gamma_e]_{z_i}|}{h} \left((|g|_{H^1(\Gamma)}^2 + k|u|_{H^1(\Gamma)}^2) + h(|g|_{H^2(\Gamma)} + k|u|_{H^2(\Gamma)}) \cdot \right. \\ &\quad \left. (|g|_{H^1(\Gamma)} + k|u|_{H^1(\Gamma)}) \right)^{1/2} \cdot \left(\|v_h\|_{L^2(\Gamma)}^2 + h\|v_h\|_{H^1(\Gamma)} \|v_h\|_{L^2(\Gamma)} \right)^{1/2} \\ &\lesssim \frac{\max_{z_i \in \Gamma \cap \mathcal{N}_h} |[\gamma_e]_{z_i}|}{h} k^{3/2} \left(\|v_h\|_0 \|v_h\|_1 + h^{1/2} \|v_h\|_1^{3/2} \|v_h\|_0^{1/2} \right)^{1/2} C_{u,g} \\ &\lesssim k \frac{\max_{z_i \in \Gamma \cap \mathcal{N}_h} |[\gamma_e]_{z_i}|}{h} \|v_h\| \|C_{u,g}\| \lesssim k h^{1+\alpha} \|v_h\| \|C_{u,g}\|, \end{aligned}$$

where we have used the second inequality in (3.6).

Since the number of the vertices of Ω is a bounded constant independent of all the parameters k , h and α , from the trace theorem we have

$$\begin{aligned} (3.16) \quad I_{2,4} &\lesssim \max_{z_i \in \mathcal{N}_h} |\gamma_e| \left\| \frac{\partial^2 u}{\partial t_e \partial n_e} \right\|_{H^1(\Gamma)}^{1/2} \left\| \frac{\partial^2 u}{\partial t_e \partial n_e} \right\|_{L^2(\Gamma)}^{1/2} \cdot \|v_h\|_{H^{1/2}(\Gamma)} \\ &\lesssim h^2 \left(\|g\|_{H^2(\Gamma)} + k\|u\|_{H^2(\Gamma)} \right)^{1/2} \left(\|g\|_{H^1(\Gamma)} + k\|u\|_{H^1(\Gamma)} \right)^{1/2} \|v_h\|_1 \\ &\lesssim k^{3/2} h^2 \|v_h\| \|C_{u,g}\|. \end{aligned}$$

Combining the inequalities (3.12)–(3.16) we have

$$(3.17) \quad |I_2| = |I_{2,1} + I_{2,2} + I_{2,3} + I_{2,4}| \lesssim (k h^{1+\alpha} + (k h)^2) \|v_h\| \|C_{u,g}\|.$$

Finally, combining the estimates of I_1 and I_2 we complete the proof. \square

Based on Lemma 3.2, we can obtain one of our main results in this paper.

THEOREM 3.3. *Assume that \mathcal{T}_h satisfies the α approximation condition. There exists a constant C_0 independent of k and h , such that if*

$$(3.18) \quad k(kh)^2 \leq C_0,$$

we have

$$(3.19) \quad |||u_h - u_I||| \lesssim (kh^{1+\alpha} + k(kh)^2) C_{u,g}.$$

Proof. For simplicity of presentation, we denote $v_h = u_h - u_I$. By the definition (2.4) and the Galerkin orthogonality, we have

$$(3.20) \quad \begin{aligned} |||u_h - u_I|||^2 &= \Re(a(u_h - u_I, v_h) + k^2(u_h - u_I, v_h)) \\ &= \Re(a(u_h - u_I, v_h) - k^2(u_h - u_I, v_h) + \mathbf{i}k \langle u_h - u_I, v_h \rangle + 2k^2(u_h - u_I, v_h)) \\ &= \Re(a(u - u_I, v_h) - k^2(u - u_I, v_h) + \mathbf{i}k \langle u - u_I, v_h \rangle + 2k^2(u_h - u_I, v_h)). \end{aligned}$$

It is well known that

$$(3.21) \quad k \|u - u_I\|_{L^2(\Omega)} \lesssim kh^2 \|u\|_{H^2(\Omega)}.$$

From Lemma 2.1, we know that there exists a constant C_0 such that if $k(kh)^2 \leq C_0$, the following inequality holds,

$$k \|u - u_h\|_{L^2(\Omega)} \lesssim ((kh)^2 + k(kh)^2) C_{u,g}.$$

Then we have

$$(3.22) \quad \begin{aligned} 2k^2(u_h - u_I, v_h) &\leq 2k \|u_h - u_I\|_{L^2(\Omega)} \cdot k \|v_h\|_{L^2(\Omega)} \\ &\leq 2 \left(k \|u - u_h\|_{L^2(\Omega)} + k \|u - u_I\|_{L^2(\Omega)} \right) \cdot k \|v_h\|_{L^2(\Omega)} \\ &\lesssim ((kh)^2 + k(kh)^2) |||v_h||| C_{u,g}. \end{aligned}$$

On the other hand, by the trace inequality,

$$(3.23) \quad \begin{aligned} |k \langle u - u_I, v_h \rangle| &\leq k \|u - u_I\|_{L^2(\partial\Omega)} \|v_h\|_{L^2(\partial\Omega)} \\ &\lesssim kh^2 \|u\|_{H^2(\partial\Omega)} \|v_h\|_{L^2(\partial\Omega)} \\ &\lesssim k^{1/2} h^2 \|u\|_{H^2(\Omega)}^{1/2} \|u\|_{H^3(\Omega)}^{1/2} |||v_h||| \\ &\lesssim (kh)^2 |||v_h||| C_{u,g}. \end{aligned}$$

Therefore, if $k(kh)^2 \leq C_0$, by Lemma 3.2 and (3.20)–(3.23), we have

$$\begin{aligned} |||u_h - u_I|||^2 &\leq |a(u - u_I, v_h)| + |k^2(u - u_I, v_h)| \\ &\quad + |k \langle u - u_I, v_h \rangle| + |2k^2(u_h - u_I, v_h)| \\ &\lesssim ((kh)^2 + kh^{1+\alpha}) |||v_h||| C_{u,g} + (kh)^2 |||v_h||| C_{u,g} \\ &\quad + ((kh)^2 + k(kh)^2) |||v_h||| C_{u,g} \\ &\lesssim (kh^{1+\alpha} + (kh)^2 + k(kh)^2) |||v_h||| C_{u,g} \\ &\lesssim (kh^{1+\alpha} + k(kh)^2) |||v_h||| C_{u,g}. \end{aligned}$$

This completes the proof. \square

4. The gradient recovery operator G_h and its superconvergence. In this section, we apply a gradient recovery operator developed in 2004, called polynomial preserving recovery (PPR) [30, 38, 40], to improve the finite element solution. We first introduce the gradient recovery operator $G_h : C(\Omega) \mapsto V_h \times V_h$. Given a node $z \in \mathcal{N}_h$, we select $n \geq 6$ sampling points $z_j \in \mathcal{N}_h$, $j = 1, 2, \dots, n$, in an element patch ω_z containing z (z is one of z_j) and fit a polynomial of degree 2, in the least squares sense, with values of u_h at those sampling points. First, we find $p_2 \in P_2(\omega_z)$ for some $w \in C(\Omega)$ such that

$$(4.1) \quad \sum_{j=1}^n (p_2 - w)^2(z_j) = \min_{q \in P_2} \sum_{j=1}^n (q - w)^2(z_j).$$

Here $P_2(\omega_z)$ is the well-known piecewise quadratic polynomial space defined on ω_z . The recovery gradient at z is then defined as

$$(4.2) \quad G_h w(z) = (\nabla p_2)(z).$$

For the linear element, the above least squares fitting procedure has a unique solution as long as those n sampling points are not on the same conic curve [30].

Now we show some properties of the gradient recovery operator G_h :

- (i) $\|G_h v_h\|_0 \lesssim \|\nabla v_h\|_0 \quad \forall v_h \in V_h$.
- (ii) For any nodal point z , $(G_h p)(z) = \nabla p(z)$ if $p \in P_j(\omega_z)$, $j = 1, 2$.
- (iii) $G_h w = G_h I_h^j w \quad \forall w \in C(\Omega)$, $j = 1, 2$.

Here $I_h^j w$ ($j = 1, 2$) are the linear nodal value interpolant and quadratic nodal value interpolant of w , respectively. The reader is referred to [30, 34, 38, 40] for more details of these properties.

From (i), we know that

$$(4.3) \quad \begin{aligned} \|G_h u_h - \nabla u\|_0 &\leq \|G_h u_h - G_h u_I\| + \|G_h u_I - \nabla u\|_0 \\ &\lesssim \|\nabla(u_h - u_I)\|_0 + \|G_h u_I - \nabla u\|_0. \end{aligned}$$

Here u_I is the linear interpolant of u . The estimate for the first term of the right hand side of the inequality (4.3) follows from Theorem 3.3. Next we will estimate the second term.

LEMMA 4.1. *For any element $\tau \in \mathcal{T}_h$ and any function $\phi \in H^3(\tilde{\tau})$,*

$$(4.4) \quad \|G_h \phi_I - \nabla \phi\|_{L^2(\tau)} \lesssim h^2 \|\phi\|_{H^3(\tilde{\tau})},$$

where $\tilde{\tau} = \bigcup \{\omega_z : z \in \mathcal{N}_h \cap \tau\}$ and ϕ_I is the linear interpolant of ϕ .

Proof. By the property (iii),

$$(4.5) \quad \|G_h \phi_I - \nabla \phi\|_{L^2(\tau)} = \|G_h \phi - \nabla \phi\|_{L^2(\tau)} = \|G_h I_h^2 \phi - \nabla \phi\|_{L^2(\tau)}.$$

For any $\eta \in P_2(\tilde{\tau})$, from the property (ii) and the fact that $G_h \eta \in V_h \times V_h$ and $\nabla \eta \in P_1(\tilde{\tau}) \times P_1(\tilde{\tau})$, it is easy to get that $G_h \eta = \nabla \eta$ in τ , which implies

$$(4.6) \quad \begin{aligned} \|G_h I_h^2 \phi - \nabla \phi\|_{L^2(\tau)} &= \|G_h (I_h^2 \phi - \eta) - \nabla(\phi - \eta)\|_{L^2(\tau)} \\ &\leq \|G_h (I_h^2 \phi - \eta)\|_{L^2(\tau)} + \|\nabla(\phi - \eta)\|_{L^2(\tau)}. \end{aligned}$$

By the definition and properties of G_h ,

$$\begin{aligned}
 (4.7) \quad \|G_h(I_h^2\phi - \eta)\|_{L^2(\tau)} &\lesssim h \max_{z \in \mathcal{N}_h \cap \tau} |G_h(I_h^2\phi - \eta)(z)| \lesssim h \|\nabla(I_h^2\phi - \eta)\|_{L^\infty(\bar{\tau})} \\
 &\lesssim \|\nabla(I_h^2\phi - \eta)\|_{L^2(\bar{\tau})} \lesssim \|\nabla(I_h^2\phi - \phi)\|_{L^2(\bar{\tau})} + \|\nabla(\phi - \eta)\|_{L^2(\bar{\tau})}.
 \end{aligned}$$

Then, from (4.5)–(4.7) we have

$$(4.8) \quad \|G_h I_h^2\phi - \nabla\phi\|_{L^2(\tau)} \lesssim \inf_{\eta \in P_2(\bar{\tau})} \|\nabla(\phi - \eta)\|_{L^2(\bar{\tau})} + \|\nabla(I_h^2\phi - \phi)\|_{L^2(\bar{\tau})}.$$

By the Hilbert–Bramble lemma and the scaling argument,

$$(4.9) \quad \inf_{\eta \in P_2(\bar{\tau})} \|\nabla(\phi - \eta)\|_{L^2(\bar{\tau})} \lesssim h^2 \|\phi\|_{H^3(\bar{\tau})},$$

and from the approximation theory

$$(4.10) \quad \|\nabla(I_h^2\phi - \phi)\|_{L^2(\bar{\tau})} \lesssim h^2 \|\phi\|_{H^3(\bar{\tau})}.$$

The proof is completed by combining (4.5) with (4.8)–(4.10) \square

The following theorem is devoted to the estimate of the second term of (4.3). In fact, it shows the superconvergence property of G_h in $H^3(\Omega)$ space for the linear element.

THEOREM 4.2. *We have the following estimate:*

$$(4.11) \quad \|G_h u_I - \nabla u\|_0 \lesssim (kh)^2 C_{u,g}.$$

Proof. From Lemma 4.1 we have

$$\begin{aligned}
 \|G_h u_I - \nabla u\|_0 &= \left(\sum_{\tau \in \mathcal{M}_h} \|G_h u_I - \nabla u\|_{L^2(\tau)}^2 \right)^{1/2} \lesssim h^2 \left(\sum_{\tau \in \mathcal{M}_h} \|u\|_{H^3(\bar{\tau})}^2 \right)^{1/2} \\
 &\lesssim h^2 \|u\|_3 \lesssim (kh)^2 C_{u,g}.
 \end{aligned}$$

\square

The following preasymptotic superconvergence estimate of the gradient recovery operator G_h can be proved by combining (4.3), Theorem 3.3 and Theorem 4.2.

THEOREM 4.3. *Assume that \mathcal{T}_h satisfies the α approximation condition. Let u and u_h be the solutions to (1.1)–(1.2) and (2.2), respectively. Then there exists a constant C_0 independent of k and h such that if $k(kh)^2 \leq C_0$,*

$$(4.12) \quad \|G_h u_h - \nabla u\|_0 \lesssim (kh^{1+\alpha} + k(kh)^2) C_{u,g}.$$

Remark 4.1. From Lemma 2.1 we know that

$$(4.13) \quad \|\nabla u_h - \nabla u\|_0 \lesssim (kh + k(kh)^2) C_{u,g}.$$

We can find that the pollution error of the finite element solution is $C_1 k(kh)^2$ from (4.13) and that of the gradient recovery operator G_h is $C_2 k(kh)^2$ from (4.12), where C_1 and C_2 are two constants independent of k and h . It is interesting that the orders of these pollution errors are the same. It seems that the gradient recovery operator does not reduce the pollution error based on our analysis. Indeed, our numerical tests in section 6 indicate that the pollution error is the same with or without the gradient recovery. In the next section, We will provide some explanation.

5. The estimate between $G_h u_h$ and ∇u_h . In this section, we devote estimating the norm $\|G_h u_h - \nabla u_h\|_0$, which motivate us to combine the PPR method and the Richardson extrapolation and define the a posteriori error estimator shown in the subsection 6.2. First, we define an elliptic projection $P_h : V \rightarrow V_h$: find $P_h u \in V_h$ such that

$$(5.1) \quad a(P_h u, v_h) + \mathbf{i}k \langle P_h u, v_h \rangle = a(u, v_h) + \mathbf{i}k \langle u, v_h \rangle \quad \forall v_h \in V_h.$$

In other words, the elliptic projection $P_h u$ of u is the finite element approximation to the solution of the following (complex-valued) Poisson problem:

$$(5.2) \quad -\Delta u = F \quad \text{in } \Omega,$$

$$(5.3) \quad \frac{\partial u}{\partial n} + \mathbf{i}k u = g \quad \text{on } \Gamma,$$

for some given function F which are determined by u . This kind of elliptic projection is often used to study some properties, such as stability and convergence, of the FEM for the Helmholtz problem. Readers are referred to [42, 41, 16, 15].

LEMMA 5.1. Assume that u is H^2 -regular. u_h^+ is its elliptic projection defined by (5.1). There hold the following estimates:

$$(5.4) \quad \|u - P_h u\| \lesssim \inf_{v_h \in V_h} \|u - v_h\|,$$

$$(5.5) \quad \|u - P_h u\|_{L^2(\Omega)} \lesssim h \inf_{v_h \in V_h} \|u - v_h\|.$$

Proof. From Lemma 3.5 in [42], we know that

$$\begin{aligned} \|u - P_h u\|_1 &\lesssim \inf_{v_h \in V_h} \left(\|u - v_h\|_1^2 + k \|u - v_h\|_{L^2(\Gamma)}^2 \right)^{1/2}, \\ \|u - P_h u\|_0 &\lesssim h \inf_{v_h \in V_h} \left(\|u - v_h\|_1^2 + k \|u - v_h\|_{L^2(\Gamma)}^2 \right)^{1/2}. \end{aligned}$$

Then the estimates (5.4)–(5.5) follow from

$$\begin{aligned} k \|u - v_h\|_{L^2(\Gamma)}^2 &\lesssim k \|u - v_h\|_0 \|u - v_h\|_1 \\ &\lesssim k^2 \|u - v_h\|_0^2 + \|u - v_h\|_1^2 \lesssim \|u - v_h\|^2. \end{aligned}$$

□

LEMMA 5.2. Assume that \mathcal{T}_h satisfies the α approximation condition and u is the exact solution to (1.1)–(1.2). $P_h u$ is its elliptic projection defined by (5.1) and u_I is its linear interpolation. We have

$$(5.6) \quad \|\nabla P_h u - \nabla u_I\|_0 \lesssim (kh^{1+\alpha} + (kh)^2) C_{u,g}.$$

Proof. Denote $v_h = P_h u - u_I$. By the Galerkin orthogonality,

$$\begin{aligned} (5.7) \quad \|P_h u - u_I\|^2 &\lesssim \Re(a(P_h u - u_I, v_h) + \mathbf{i}k \langle P_h u - u_I, v_h \rangle) + k^2 (P_h u - u_I, v_h) \\ &\lesssim \Re(a(u - u_I, v_h) + \mathbf{i}k \langle u - u_I, v_h \rangle) + k^2 (P_h u - u_I, v_h) \\ &\lesssim |a(u - u_I, v_h)| + |k \langle u - u_I, v_h \rangle| + k \|P_h u - u_I\|_0 \cdot k \|v_h\|_0. \end{aligned}$$

Then the estimate (5.6) follows from Lemma 3.2, (3.23) and the fact that

$$\begin{aligned} k \|u_h^+ - u_I\|_0 \cdot k \|v_h\|_0 &\leq (k \|u_h^+ - u\|_0 + k \|u - u_I\|_0) \|v_h\|_{1,h} \\ &\lesssim (kh)^2 (1 + \sqrt{kh}) \|v_h\|_{1,h} C_{u,g}. \end{aligned}$$

□

Similar to (4.3), we have

$$(5.8) \quad \|G_h P_h u - \nabla u\|_0 \lesssim \|\nabla(P_h u - u_I)\|_0 + \|G_h u_I - \nabla u\|_0.$$

Then from Lemma 5.2, Theorem 4.2 and (5.8), we can obtain the following theorem.

THEOREM 5.3. *Assume that \mathcal{T}_h satisfies the α approximation condition. Let u and $P_h u$ be the solutions to (1.1)–(1.2) and (5.1), respectively. Then the following error estimate holds:*

$$(5.9) \quad \|G_h P_h u - \nabla u\|_0 \lesssim (kh^{1+\alpha} + (kh)^2) C_{u,g}.$$

From Lemma 5.1, we see that the elliptic projection of u is not *polluted*. As a result, the second term on the right-hand side of the estimate (5.9) is $(kh)^2$ instead of $k(kh)^2$. Furthermore, the error estimate of the elliptic projection of u does not require the mesh condition $k(kh)^2 \leq C_0$.

THEOREM 5.4. *Assume that \mathcal{T}_h satisfies the α approximation condition. Let u_h be the linear finite element solution to the problem (1.1)–(1.2). We have*

$$(5.10) \quad \|G_h u_h - \nabla u_h\|_0 \lesssim (kh + k(kh)^3) C_{u,g}.$$

Proof. We write $u_h = P_h u + (u_h - P_h u) := P_h u + \theta_h$, where $P_h u$ is defined by (5.1). Then by the triangle inequality we have

$$(5.11) \quad \begin{aligned} \|G_h u_h - \nabla u_h\|_0 &= \|G_h(P_h u + \theta_h) - \nabla(P_h u + \theta_h)\|_0 \\ &\lesssim \|G_h P_h u - \nabla P_h u\|_0 + \|G_h \theta_h - \nabla \theta_h\|_0. \end{aligned}$$

From Lemma 5.1,

$$\begin{aligned} \|\nabla u - \nabla P_h u\|_0^2 &\lesssim \inf_{v_h \in V_h} \|u - v_h\|^2 \lesssim |u - u_I|_1^2 + k^2 \|u - u_I\|_0^2 \\ &\lesssim h^2 (1 + k^2 h^2) \|u\|_2^2 \lesssim (kh)^2 (1 + (kh)^2) C_{u,g}^2, \end{aligned}$$

which implies that from Theorem 5.3,

$$(5.12) \quad \begin{aligned} \|G_h P_h u - \nabla P_h u\|_0 &\leq \|G_h P_h u - \nabla u\|_0 + \|\nabla u - \nabla P_h u\|_0 \\ &\lesssim (kh^{1+\alpha} + (kh)^2) C_{u,g} + kh C_{u,g} \\ &\lesssim (kh + (kh)^2) C_{u,g}. \end{aligned}$$

From (2.2) and (5.1), we see that θ_h satisfies

$$(5.13) \quad a(\theta_h, v_h) + \mathbf{i}k \langle \theta_h, v_h \rangle = -k^2 (u - u_h, v_h).$$

It is easy to see that θ_h can be understood as the finite element solution to the following Poisson problem with Robin boundary:

$$\begin{aligned} -\Delta\theta &= -k^2(u - u_h) \quad \text{in } \Omega, \\ \frac{\partial\theta}{\partial n} + \mathbf{i}k\theta &= 0 \quad \text{on } \Gamma. \end{aligned}$$

Therefore,

$$\begin{aligned} (5.14) \quad \|G_h\theta_h - \nabla\theta_h\|_0 &\leq \|G_h\theta_h - \nabla\theta\|_0 + \|\nabla\theta - \nabla\theta_h\|_0 \\ &\lesssim h\|\theta\|_2 \lesssim k^2h\|u - u_h\|_0 \\ &\lesssim k^2h(kh^2 + k^2h^2)C_{u,g} \\ &\lesssim ((kh)^3 + k(kh)^3)C_{u,g}. \end{aligned}$$

The proof is completed by combining (5.11)–(5.14). \square

Remark 5.1. We emphasize that the estimate of $\|G_hu_h - \nabla u_h\|_0$ may not be perfect, although $k(kh)^3$ is less than the pollution error $k(kh)^2$ of the operator G_h . What we expect is the estimate $\|G_hu_h - \nabla u_h\|_0 \lesssim khC_{u,g}$, which coincides with our numerical tests in the next section. However, if invoking the mesh condition $k(kh)^2 \leq C_0$, we have $\|G_hu_h - \nabla u_h\|_0 \lesssim kh(1 + C_0)C_{u,g}$, which indicates that the pollution error between these two quantities are “almost” cancelled.

6. Numerical examples. In this section, we will verify our theoretical results by simulating the following two-dimensional Helmholtz problem:

$$(6.1) \quad -\Delta u - k^2u = f := \frac{\sin(kr)}{r} \quad \text{in } \Omega,$$

$$(6.2) \quad \frac{\partial u}{\partial n} + \mathbf{i}ku = g \quad \text{on } \Gamma.$$

g is so chosen that the exact solution is

$$(6.3) \quad u = \frac{\cos(kr)}{r} - \frac{\cos k + \mathbf{i} \sin k}{k(J_0(k) + \mathbf{i}J_1(k))} J_0(kr)$$

in polar coordinates, where $J_\nu(z)$ are Bessel functions of the first kind.

This problem has been computed in [18, 15, 41, 16] by the finite element method, the continuous interior penalty finite element method and the interior penalty discontinuous Galerkin method on both triangular meshes and rectangular meshes.

6.1. Errors of ∇u_h and G_hu_h . Let Ω be the unit regular hexagon with center (0,0) (cf. Figure 6). For any positive integer m , let $\mathcal{T}_{1/m}$ be the regular triangulation that consists of $6m^2$ congruent and equilateral triangles of size $h = 1/m$. See Figure 6 for a sample triangulation $\mathcal{T}_{1/5}$. Let u_h be the linear finite element solution in this subsection.

From Theorem 4.3, the error of the recovered gradient in the H^1 -seminorm is bounded by

$$(6.4) \quad \|G_hu_h - \nabla u\|_0 \leq C_1kh^{1+\alpha} + C_2k(kh)^2$$

for some constants C_1 and C_2 if $k(kh)^2 \leq C_0$. The second term on the right-hand side of (6.4) is the so-called pollution error. We actually have $\alpha = 1$ because of the

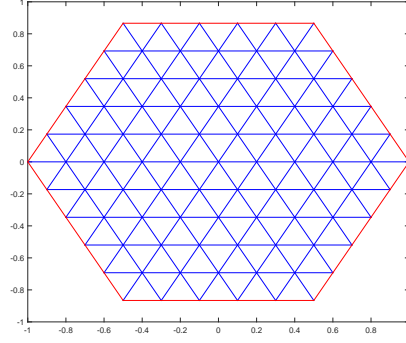


FIG. 6.1. Geometry and a sample mesh $\mathcal{T}_{1/5}$ that consists of congruent and equilateral triangles of size $h = 1/5$ for the example.

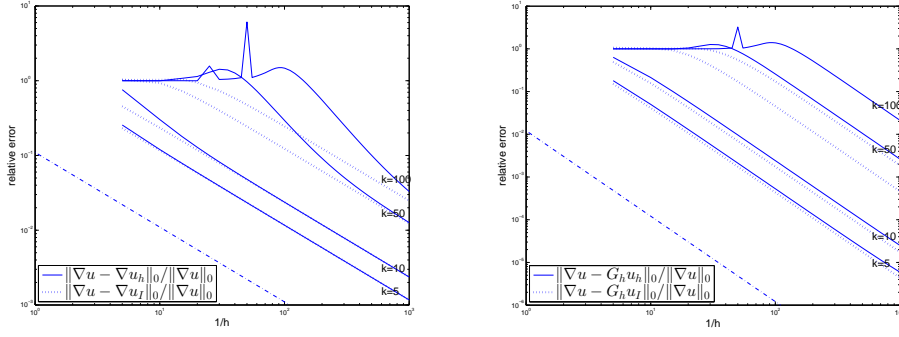


FIG. 6.2. Left graph: the relative error of the finite element solution (solid) and the relative error of the finite element interpolant (dotted) in H^1 -seminorm for $k = 5, k = 10, k = 50$, and $k = 100$, respectively. Right graph: the relative error of the recovered gradient of the finite element solution and that of the finite element interpolant for $k = 5, k = 10, k = 50$, and $k = 100$, respectively. Dash-dot lines give reference slopes -1 and -2 , respectively.

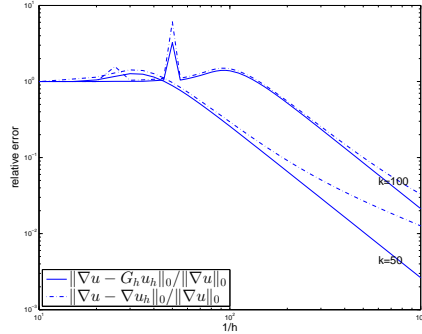


FIG. 6.3. The relative error of the finite element solution (dash-dot) and that of the recovered gradient of the finite element solution (solid).

congruent and equilateral triangles in the meshes (see Figure 6). We now verify the error bound by numerical results.

In the left graph of Figure 6.2, the H^1 -seminorm relative error of the finite element solution and that of the linear interpolant are displayed simultaneously. When $k = 5, 10$, the relative error of the finite element solution is similar to that of the interpolant. When $k = 50, 100$, we can easily detect the existence of the pollution error and the effect of the mesh condition $k(kh)^2 \leq C_0$. By contrast, as shown in the right graph of Figure 6.2, the gradient recovery method converges faster than the linear interpolant and the relative error of the recovered gradient decays at rate h^2 (slope -2 in the log-log scale) for $k = 5, 10$. For $k = 50, 100$, the relative error of the recovered gradient stays around 100% (no-convergence) and then decays at rate h^2 . We notice that the “no-convergence range” increases with k . In addition, Figure 6.3 shows that the decaying points of both the gradient of the finite element solution ∇u_h and the recovered gradient $G_h u_h$ are the same, which indicates that their convergence mesh conditions are the same, that is $k(kh)^2 \leq C_0$, and the pollution effect is still there for the recovered gradient. We remark that the numerical tests for the pollution phenomenon of the finite element method have been done largely in the literature. For more details, a reader is refer to [15] and references therein.

Next we verify more precisely the pollution term in (6.4). To do so, we introduce the definition of the critical mesh size with respect to a given relative tolerance [33, 15].

DEFINITION 6.1. *Given a relative tolerance ε , a wave number k , the critical mesh size $h(k, \varepsilon)$ with respect to the relative tolerance ε is defined by the maximum mesh size such that the relative error of the finite element solution in the H^1 -seminorm (or the relative error of recovered gradient of the finite element solution in the H^0 -norm) is less than or equal to ε*

Clearly, if the pollution terms in (4.13) and (6.4) are of order $k^3 h^2$, then $h(k, \varepsilon)$ should be proportional to $k^{-3/2}$ for k large enough. This is verified by Figure 6.4. So our theoretical result is sharp with respect to k and h .

To compare the pollution errors more intuitively, we plot the relative error of the finite element solution in the H^1 -seminorm and the relative error of the recovered gradient in the H^0 -norm for $k = 1, 2, \dots, 600$ with fixed $kh = 1$ and $kh = 1/2$ in the left graph of Figure 6.5. We see that both relative errors increase linearly in the pre-asymptotical range $k(kh)^2 \leq C_0$: for $kh = 1/2$, the range is about $k \leq 500$, and for $kh = 1$, the range is much less with $k \leq 100$. However, we do not know the behaviors of these relative errors when k is much larger theoretically.

To investigate further the influence of PPR to the pollution errors, we estimate the error between the gradient of the finite element solution and its recovered gradient and prove that this error is controlled by $(kh + k(kh)^3)C_{u,g}$ (cf. Theorem 5.4). In the right graph of Figure 6.5, we depict this error for $kh = 1$ and $kh = 1/2$, respectively. We see that both of them are dominated by kh , which indicates that the pollution error is “almost” cancelled between the gradient of the finite element solution and its recovered gradient. So our estimate in Theorem 5.4 is pre-asymptotically correct under the mesh condition $k(kh)^2 \leq C_0$. However, the relative error estimate under other mesh condition is still unknown and deserves further study in the future.

Both graphs of Figure 6.5 imply that the gradient recovery method does not reduce the pollution error of the finite element solution. Nevertheless, it does improve the low order term in (4.13).

6.2. Richardson extrapolation and the a posteriori error estimator. The Richardson extrapolation method is an efficient procedure to raise the accuracy of

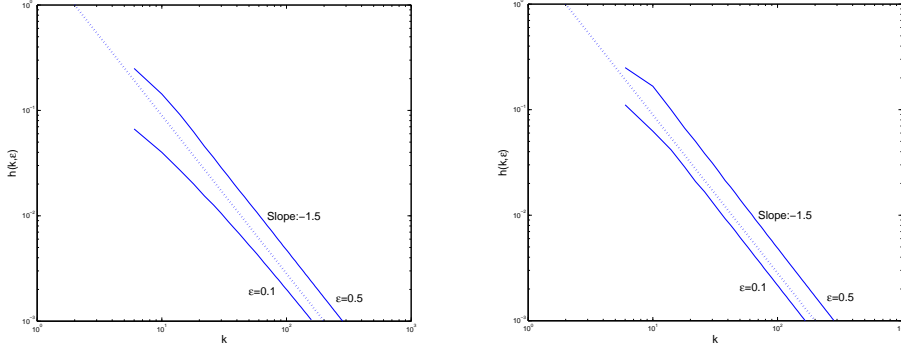


FIG. 6.4. $h(k, 0.5)$ and $h(k, 0.1)$ versus k for the finite element solution (left) and for the recovered gradient of the finite element solution (right), respectively. The dotted lines give lines of slope -1.5 in the log-log scale.

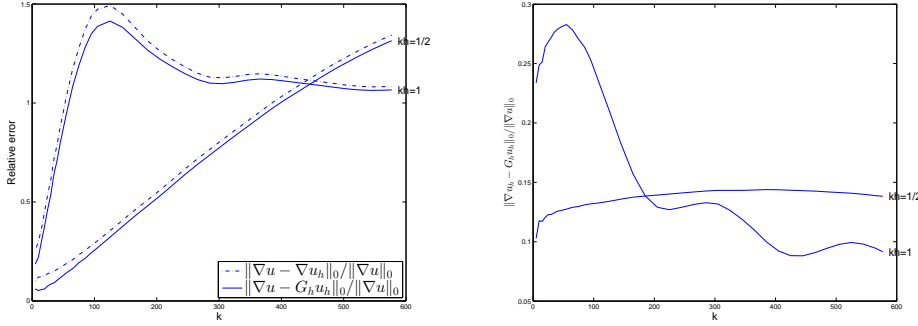


FIG. 6.5. Left graph: the relative error of the finite element solution in H^1 -seminorm (dash-dot lines) and that of the recovered gradient of the finite element solution in H^0 -norm (solid lines) with mesh size h determined by $kh = 1$ and $kh = 1/2$. Right graph: the estimate between $G_h u_h$ and ∇u_h with mesh size h determined by $kh = 1$ and $kh = 1/2$.

numerical methods, such as finite difference [26] and finite element methods [7, 32, 21, 25]. In this subsection, we apply the Richardson extrapolation to the gradient and recovered gradient of the finite element solution, respectively. Our motivation is based on the error estimate (4.12) in Theorem 4.3. With $\alpha = 1$, both the interpolation error and pollution error are of order h^2 (with different powers of k), and hence Richardson extrapolation would work on both terms simultaneously. Since the powers of h in the two terms of (4.13) are not balanced, the Richardson extrapolation will not work without using PPR recovery. Our numerical tests clearly demonstrate this difference as we shall see in the subsequence.

Let \mathcal{T}_h be a uniform and regular triangulation and let $\mathcal{T}_{h/2}$ be generated from \mathcal{T}_h by dividing each triangle as usual into four congruent subtriangles.

Define the Richardson extrapolation operator R by

$$Rv_{h/2}|_K = (4v_{h/2} - v_h)/3 \quad \forall K \in \mathcal{T}_{h/2},$$

where v_h is a piecewise polynomial function over \mathcal{T}_h .

h	∇u_h	$R\nabla u_h$	$G_h u_h$	$RG_h u_h$	$G_h u_I$
1/4	9.5808e-01		9.5511e-01		
1/8	5.8248e-01	6.0502e-01	5.3014e-01	4.5896e-01	3.9074e-01
1/16	2.6521e-01	2.6763e-01	1.8339e-01	9.4611e-02	1.1620e-01
1/32	1.2121e-01	1.3214e-01	5.0599e-02	1.2457e-02	2.9841e-02
1/64	5.8610e-02	6.6580e-02	1.2986e-02	2.1927e-03	7.4567e-03
1/128	2.9033e-02	3.3383e-02	3.2693e-03	5.0283e-04	1.8578e-03
1/256	1.4482e-02	1.6704e-02	8.1935e-04	1.2149e-04	4.6332e-04
1/512	7.2365e-03	8.3538e-03	2.0524e-04	2.9832e-05	1.1566e-04
1/1024	3.6177e-03	4.1771e-03	5.1531e-05	7.4156e-06	2.8894e-05

TABLE 6.1

$\|\nabla u - \nabla u_h\|_0 / |u|_1$, $\|\nabla u - R\nabla u_h\|_0 / |u|_1$, $\|\nabla u - G_h u_h\|_0 / |u|_1$, $\|\nabla u - RG_h u_h\|_0 / |u|_1$ and $\|\nabla u - G_h u_I\|_0 / |u|_1$ over \mathcal{T}_h for $k = 10$.

h	∇u_h	$R\nabla u_h$	$G_h u_h$	$RG_h u_h$	$G_h u_I$
1/4	9.9910e-01		9.9873e-01		
1/8	1.0048e+00	1.0087e+00	1.0056e+00	1.0096e+00	1.0055e+00
1/16	1.0693e+00	1.1290e+00	9.9738e-01	1.0036e+00	1.0014e+00
1/32	1.1929e+00	1.3541e+00	1.0570e+00	1.1145e+00	5.9028e-01
1/64	1.1021e+00	1.3134e+00	1.0128e+00	1.1568e+00	1.8951e-01
1/128	3.9158e-01	3.9411e-01	3.5433e-01	3.2505e-01	5.0046e-02
1/256	1.2126e-01	9.5288e-02	9.2998e-02	2.9092e-02	1.2631e-02
1/512	4.5197e-02	4.4683e-02	2.3462e-02	2.0761e-03	3.1591e-03
1/1024	2.0172e-02	2.2284e-02	5.8762e-03	2.2653e-04	7.8911e-04

TABLE 6.2

$\|\nabla u - \nabla u_h\|_0 / |u|_1$, $\|\nabla u - R\nabla u_h\|_0 / |u|_1$, $\|\nabla u - G_h u_h\|_0 / |u|_1$, $\|\nabla u - RG_h u_h\|_0 / |u|_1$ and $\|\nabla u - G_h u_I\|_0 / |u|_1$ over \mathcal{T}_h for $k = 50$.

We first simulate the problem (6.1)–(6.2) over regular pattern uniform triangulations \mathcal{T}_h of the unit square $[0, 1] \times [0, 1]$.

Table 6.1 shows the relative L^2 -norm errors of ∇u_h , $R\nabla u_h$ and their Richardson extrapolation in the case $k = 10$. As we expected, $\|\nabla u - \nabla u_h\|_0 / |u|_1$ converges at rate $O(h)$ and $\|\nabla u - G_h u_h\|_0 / |u|_1$ decays at rate $O(h^2)$. We can observe that the relative error of $R\nabla u_h$ is worse than that of ∇u_h and the relative error of $RG_h u_h$ is much better than that of $G_h u_h$. For a larger wave number $k = 50$, the relative errors are shown in Table 6.2. The data demonstrate similar behaviors of numerical solutions to those in Table 6.1 when the mesh size is sufficient small.

The good behavior of the operator RG_h in Table 6.1 and Table 6.2 makes it possible to define the following *a posteriori* error estimator

$$(6.5) \quad \eta_h = \|RG_h u_h - \nabla u_h\|_0.$$

Table 6.3 and Table 6.4 illustrate the asymptotic exactness of the error estimator based on the recovery operator G_h and the extrapolation operator R .

Next we turn to the Delaunay triangulation over the unit square Ω and L-shaped domain $\Omega_L = \Omega \setminus [0.5, 1] \times [0.5, 1]$. The initial mesh \mathcal{T}_0^D is obtained by using a Delaunay triangulation algorithm. Then \mathcal{T}_j^D is obtained from \mathcal{T}_{j-1}^D by dividing each triangle

	k=10		k=30	
h	$\ \nabla u - \nabla u_h\ _0$	η_h	$\ \nabla u - \nabla u_h\ _0$	η_h
1/4	7.9165e-01		8.9499e-01	
1/8	4.8127e-01	3.5128e-01	8.8726e-01	2.8705e-01
1/16	2.1913e-01	1.9677e-01	9.9983e-01	4.2429e-01
1/32	1.0015e-01	9.8802e-02	7.9908e-01	3.1293e-01
1/64	4.8426e-02	4.8414e-02	2.9350e-01	2.2032e-01
1/128	2.3988e-02	2.3994e-02	1.0199e-01	9.7829e-02
1/256	1.1965e-02	1.1966e-02	4.2406e-02	4.2259e-02
1/512	5.9791e-03	5.9793e-03	1.9948e-02	1.9945e-02
1/1024	2.9891e-03	2.9891e-03	9.8094e-03	9.8098e-03

TABLE 6.3

The errors of ∇u_h and the a posteriori error estimator over \mathcal{T}_h for $k = 10$ and $k = 30$

	k=60		k=120	
h	$\ \nabla u - \nabla u_h\ _0$	η_h	$\ \nabla u - \nabla u_h\ _0$	η_h
1/4	8.3466e-01		8.2188e-01	
1/8	8.8755e-01	6.1990e-02	8.5109e-01	1.5580e-02
1/16	9.0952e-01	2.8306e-01	8.7877e-01	4.7890e-02
1/32	9.9385e-01	3.7793e-01	9.2054e-01	2.9554e-01
1/64	1.1260e+00	2.9684e-01	9.8618e-01	3.4281e-01
1/128	5.4450e-01	3.1504e-01	1.0975e+00	2.6629e-01
1/256	1.6186e-01	1.4898e-01	9.6799e-01	3.3001e-01
1/512	5.3586e-02	5.3062e-02	3.0027e-01	2.5931e-01
1/1024	2.1947e-02	2.1932e-02	8.3593e-02	8.2496e-02

TABLE 6.4

The errors of ∇u_h and the a posteriori error estimates over \mathcal{T}_h for $k = 60$ and $k = 120$

into four congruent triangles. Data in Tables 6.5–6.8 show the superconvergence of the recovered gradient at the rate of $O(h^2)$ (see the fourth columns) and the asymptotic exactness of η_h (see the sixth columns) over Delaunay triangulations. Therefore, the PPR method combined with the Richardson extrapolation performs very well and leads to an a posteriori error estimator.

Finally, we use the a posteriori error estimator (6.5) to simulate the Helmholtz problem

$$(6.6) \quad -\Delta u - k^2 u = \frac{\sin(k\tilde{r})}{\tilde{r}} e^{-50\tilde{r}} \quad \text{in } \Omega,$$

$$(6.7) \quad \frac{\partial u}{\partial n} + \mathbf{i}ku = 0 \quad \text{on } \Gamma,$$

where Ω is the unit square $[0, 1] \times [0, 1]$ and $\tilde{r} = \sqrt{(x - 0.5)^2 + (y - 0.5)^2}$. Let u_h be the linear finite element solution to the problem (6.6)–(6.7) over \mathcal{T}_m .

We do not have the expression of the exact solution to the problem (6.6)–(6.7). However, Table 6.9 shows that the solutions are relatively accurate when the mesh sizes are greater than 128, 512, 1024 for the wave numbers $k = 30, 60, 120$, respectively.

m	DOF	$\ \nabla u - \nabla u_h\ _0$	$\ \nabla u - G_h u_h\ _0$	$\ \nabla u - RG_h u_h\ _0$	η_h
0	54	4.1028e-01	4.2562e-01		
1	193	1.8409e-01	1.4508e-01	8.2579e-02	1.8430e-01
2	729	8.7025e-02	3.8073e-02	1.2520e-02	8.7486e-02
3	2833	4.2749e-02	9.4214e-03	2.6138e-03	4.2840e-02
4	11169	2.1275e-02	2.3269e-03	5.7444e-04	2.1286e-02
5	44353	1.0625e-02	5.7802e-04	1.3013e-04	1.0626e-02
6	176769	5.3111e-03	1.4423e-04	3.0557e-05	5.3112e-03
7	705793	2.6553e-03	3.6082e-05	7.3719e-06	2.6554e-03

TABLE 6.5

The errors of ∇u_h , $G_h u_h$, $RG_h u_h$ and the *a posteriori* error estimates over the Delaunay triangulation \mathcal{T}_m^D of the unit square Ω ($m = 0, 1, 2, \dots, 7$) for $k = 10$.

m	DOF	$\ \nabla u - \nabla u_h\ _0$	$\ \nabla u - G_h u_h\ _0$	$\ \nabla u - RG_h u_h\ _0$	η_h
0	54	8.8926e-01	8.8934e-01		
1	193	9.4715e-01	8.7929e-01	8.8957e-01	4.0315e-01
2	729	9.4889e-01	8.7838e-01	8.9673e-01	2.9724e-01
3	2833	1.0437e+00	9.5886e-01	1.0742e+00	2.9106e-01
4	11169	3.7904e-01	3.4890e-01	3.1643e-01	2.6232e-01
5	44353	1.1633e-01	9.2797e-02	2.9542e-02	1.0972e-01
6	176769	4.2413e-02	2.3489e-02	2.3164e-03	4.2156e-02
7	705793	1.8666e-02	5.8886e-03	3.1415e-04	1.8661e-02

TABLE 6.6

The errors of ∇u_h , $G_h u_h$, $RG_h u_h$ and the *a posteriori* error estimates over the Delaunay triangulation \mathcal{T}_m^D of the unit square Ω ($m = 0, 1, 2, \dots, 7$) for $k = 60$.

The graphs of numerical solutions for different k and h in Figure 6.6–6.8 illustrate the findings.

7. Concluding Remarks. In this work, we have studied superconvergence properties of linear FEM based on PPR for the Helmholtz equation with large wave number. We analyzed (1) gradient error between the finite element solution and the linear interpolation $\|\nabla(u_h - u_I)\|_{L^2(\Omega)}$ (c.f. (3.19)) and (2) the error between the true gradient and recovered gradient from the finite element solution $\|\nabla u - G_h u_h\|_{L^2(\Omega)}$ (c.f. (4.12)) under the mesh condition $k(kh)^2 \leq C_0$ (2.2). Both errors consist of two parts $C_1 kh^{1+\alpha} + C_2 k(kh)^2$ with the first term improved by a factor h^α and the second term remained the same from the original gradient error. We see that the recovered gradient still suffers from the pollution error. We further analyzed (3) the difference between the finite element solution gradient and the recovered gradient by PPR and found that the pollution part of this error can be improved to $k(kh)^3$ (c.f. (5.10)), which implies $\|G_h u_h - \nabla u_h\|_0 \lesssim kh$ if $k(kh)^2 \leq C_0$, (see remark 5.1). In another word, $\|G_h u_h - \nabla u_h\|_0$ can not provide a good measure of the H^1 -error of the finite element solution for h in the preasymptotic range since $\|\nabla u - \nabla u_h\|_0$ contains also the pollution term. However, the superconvergence rate $O(h^2)$ of the recovered gradient makes it possible that the Richardson extrapolation improves the numerical solution further. Therefore, $\|RG_h u_h - \nabla u_h\|_0$ can measure the H^1 -error of the finite element solution very well and leads to asymptotically exact *a posteriori* error esti-

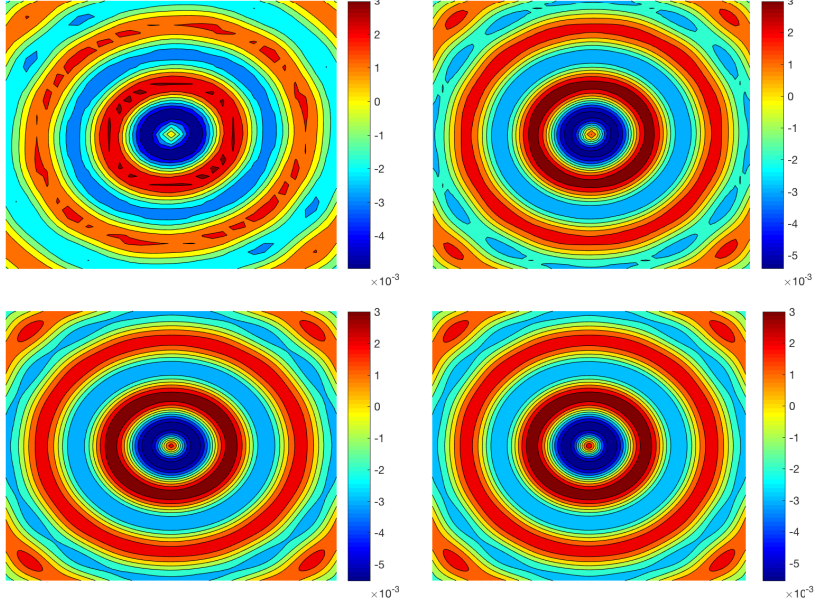


FIG. 6.6. The real part of the finite element solution for the equations (6.6)–(6.7) for $k = 30$ over \mathcal{T}_m with $m = 8$ (top left), $m = 32$ (top right), $m = 128$ (bottom left) and $m = 1024$ (bottom right).

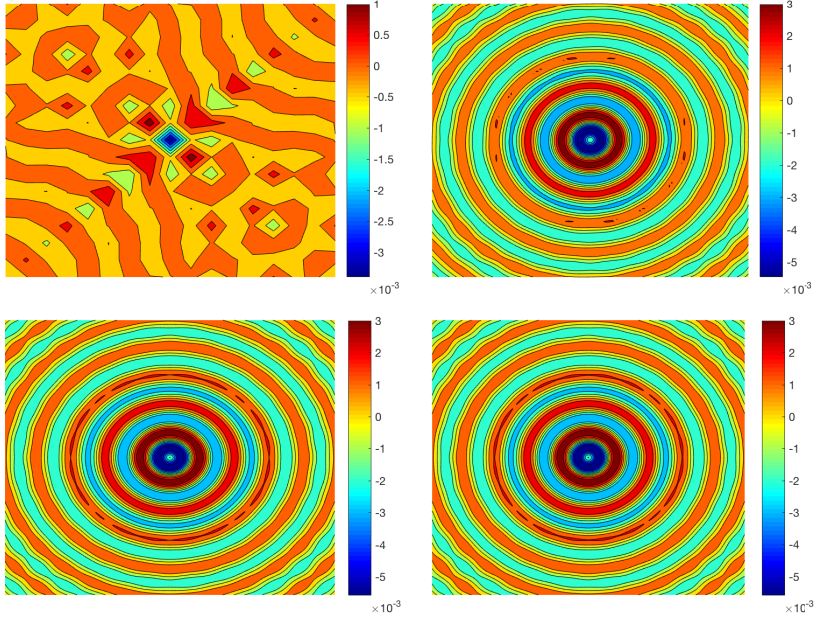


FIG. 6.7. The real part of the finite element solution for the equations (6.6)–(6.7) for $k = 60$ over \mathcal{T}_m with $m = 16$ (top left), $m = 128$ (top right), $m = 512$ (bottom left) and $m = 1024$ (bottom right).

m	DOF	$\ \nabla u - \nabla u_h\ _0$	$\ \nabla u - G_h u_h\ _0$	$\ \nabla u - RG_h u_h\ _0$	η_h
0	279	1.1742e-01	7.5574e-02		
1	1057	5.8161e-02	1.8932e-02	7.9039e-03	5.8495e-02
2	4113	2.9051e-02	4.7206e-03	1.6396e-03	2.9076e-02
3	16225	1.4529e-02	1.1963e-03	3.7617e-04	1.4530e-02
4	64449	7.2656e-03	3.0479e-04	8.8224e-05	7.2656e-03
5	256900	3.6331e-03	7.7808e-05	2.1327e-05	3.6331e-03
6	1025800	1.8166e-03	1.9875e-05	5.2388e-06	1.8166e-03

TABLE 6.7

The errors of ∇u_h , $G_h u_h$, $RG_h u_h$ and the a posteriori error estimates over the Delaunay triangulation \mathcal{T}_m^D of the L-shaped domain Ω_L ($m = 0, 1, 2, \dots, 7$) for $k = 10$.

m	DOF	$\ \nabla u - \nabla u_h\ _0$	$\ \nabla u - G_h u_h\ _0$	$\ \nabla u - RG_h u_h\ _0$	η_h
0	279	9.3370e-01	8.0586e-01		
1	1057	9.9962e-01	8.9924e-01	9.6330e-01	3.0810e-01
2	4113	5.7234e-01	5.3249e-01	5.8243e-01	2.6218e-01
3	16225	1.8276e-01	1.5775e-01	8.6317e-02	1.5438e-01
4	64449	6.2328e-02	4.0796e-02	7.0117e-03	6.0954e-02
5	256900	2.5937e-02	1.0278e-02	7.4238e-04	2.5894e-02
6	1025800	1.2217e-02	2.5744e-03	1.4689e-04	1.2217e-02

TABLE 6.8

The errors of ∇u_h , $G_h u_h$, $RG_h u_h$ and the a posteriori error estimates over the Delaunay triangulation \mathcal{T}_m^D of the L-shaped domain Ω_L ($m = 0, 1, 2, \dots, 7$) for $k = 60$.

mators. All aforementioned error bounds are verified by numerical tests in Section 6. As by-products, we also estimated the following quantities: $\|G_h u_I - \nabla u\|_{L^2(\Omega)}$ (c.f. (4.11)), $\|\nabla P_h u - \nabla u_I\|_{L^2(\Omega)}$ (c.f. (5.6)), $\|G_h P_h u - \nabla u\|_{L^2(\Omega)}$ (c.f., (5.9)), and found that they have a common pollution term $(kh)^2$, which indicates that these quantities suffer much less from the pollution.

REFERENCES

- [1] COMSOL AB., *COMSOL MultiPhysics User's Guide*, 3.5a ed., 2008.
- [2] M AINSWORTH, *Discrete dispersion relation for hp-version finite element approximation at high wave number*, SIAM J. Numer. Anal., 42 (2004), pp. 553–575.
- [3] A.K. AZIZ AND R.B. KELLOGG, *A scattering problem for the Helmholtz equation*, in *Advances in Computer Methods for Partial Differential Equations-III*, vol. 1, 1979, pp. 93–95.
- [4] I. BABUŠKA, F. IHLENBURG, E.T. PAIK, AND S.A. SAUTER, *A generalized finite element method for solving the Helmholtz equation in two dimensions with minimal pollution*, Comput. Methods Appl. Mech. Engrg., 128 (1995), pp. 325–359.
- [5] I. BABUŠKA AND S.A. SAUTER, *Is the pollution effect of the FEM avoidable for the Helmholtz equation considering high wave numbers?*, SIAM Rev., 42 (2000), pp. 451–484.
- [6] R. E. BANK AND J. XU, *Asymptotically exact a posteriori error estimators, Part I: Grid with superconvergence*, SIAM J. Numer. Anal., 41 (2003), pp. 2294–2312.
- [7] H. BLUM AND R. RANNACHER, *Asymptotic error expansion and richardson extrapolation for linear finite elements*, Numer. Math., 49 (1986), pp. 11–38.
- [8] S.C. BRENNER AND L.R. SCOTT, *The mathematical theory of finite element methods*, Springer, New York, third ed., 2008.
- [9] E. BURMAN, H. WU, AND L. ZHU, *Continuous interior penalty finite element method for Helmholtz equation with high wave number: One dimensional analysis*, arXiv:1211.1424.

m	$k = 30$	$k = 60$	$k = 120$
8	5.6287e-03	1.4636e-04	6.2692e-05
16	2.0711e-02	2.1027e-02	3.6726e-04
32	2.2812e-02	4.0705e-02	3.6307e-02
64	1.4604e-02	3.6427e-02	5.1698e-02
128	7.1816e-03	2.6521e-02	4.9015e-02
256	3.4422e-03	1.2030e-02	4.3212e-02
512	1.6928e-03	5.1373e-03	2.0382e-02
1024	8.4244e-04	2.4126e-03	7.4914e-03

TABLE 6.9

The *a posteriori* error estimator η_h over \mathcal{T}_m ($m = 8, 16, \dots, 1024$) for $k = 30, 60, 120$

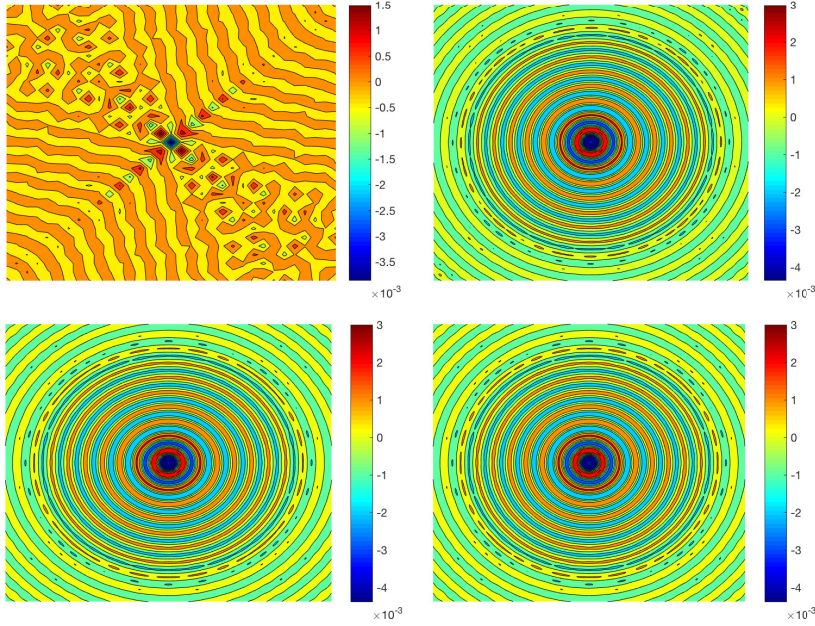


FIG. 6.8. The real part of the finite element solution for the equations (6.6)–(6.7) for $k = 120$ over \mathcal{T}_m with $m = 32$ (top left), $m = 512$ (top right), $m = 1024$ (bottom left) and $m = 2048$ (bottom right).

- [10] L. CHEN AND J. XU, *Topics on adaptive finite element methods*, in *Adaptive Computations: Theory and Algorithms*, T. Tang and J. Xu, eds., Science Press, Beijing, 2007.
- [11] Z. CHEN AND X. XIANG, *A source transfer domain decomposition method for helmholtz equations in unbounded domain*, SIAM J. Numer. Anal., 51 (2013), pp. 2331–2356.
- [12] P. G. CIARLET, *The finite element method for elliptic problems*, North-Holland Pub. Co., New York, 1978.
- [13] A. DERAEMAERKER, I. BABUŠKA, AND P. BOUILLARD, *Dispersion and pollution of the FEM solution for the Helmholtz equation in one, two and three dimensions*, Internat. J. Numer. Methods Engrg., 46 (1999), pp. 471–499.
- [14] J. DOUGLAS JR, J.E. SANTOS, AND D. SHEEN, *Approximation of scalar waves in the space-frequency domain*, Math. Models Methods Appl. Sci., 4 (1994), pp. 509–531.
- [15] Y. DU AND H. WU, *Preasymptotic error analysis of higher order FEM and CIP-FEM for Helmholtz equation with high wave number*, SIAM J. Numer. Anal., 53 (2015), pp. 782–

- 804.
- [16] Y. DU AND L. ZHU, *Preasymptotic error analysis of high order interior penalty discontinuous Galerkin methods for the Helmholtz equation with high wave number*, J. Sci. Comput., Accepted, (2015).
 - [17] B. ENGQUIST AND A. MAJDA, *Radiation boundary conditions for acoustic and elastic wave calculations*, Comm. Pure Appl. Math., 32 (1979), pp. 313–357.
 - [18] X. FENG AND H. WU, *Discontinuous Galerkin methods for the Helmholtz equation with large wave numbers*, SIAM J. Numer. Anal., 47 (2009), pp. 2872–2896.
 - [19] ———, *hp-discontinuous Galerkin methods for the Helmholtz equation with large wave number*, Math. Comp., 80 (2011), pp. 1997–2024.
 - [20] I. HARARI, *Reducing spurious dispersion, anisotropy and reflection in finite element analysis of time-harmonic acoustics*, Comput. Meth. Appl. Mech. Engrg., 140 (1997), pp. 39–58.
 - [21] P. HELFRICH, *Asymptotic expansion for the finite element approximations of parabolic problems*, Bonner Math. Schriften, 158 (1983), pp. 11–30.
 - [22] F. IHLENBURG AND I. BABUŠKA, *Finite element solution of the Helmholtz equation with high wave number. I. The h-version of the FEM*, Comput. Math. Appl., 30 (1995), pp. 9–37.
 - [23] ———, *Finite element solution of the Helmholtz equation with high wave number. II. The h-p version of the FEM*, SIAM J. Numer. Anal., 34 (1997), pp. 315–358.
 - [24] A. M. LAKHANY, I. MAREK, AND J. R. WHITEMAN, *Superconvergence results on mildly structured triangulations*, Comput. Methods Appl. Mech. Engrg., 189 (2000), pp. 1–75.
 - [25] Q. LIN, S. ZHANG, AND N. YAN, *Asymptotic error expansion and defect correction for Sobolev and viscoelasticity type equations*, J. Comput. Math., 16 (1998), pp. 57–62.
 - [26] G. MARCHUK AND V. SHAIUROV, *Difference Methods and Their Extrapolation*, Springer-Verlag, New York, 1983.
 - [27] JM MELENK, A PARSANIA, AND S SAUTER, *General DG-methods for highly indefinite Helmholtz problems*, Journal of Scientific Computing, 57 (2013), pp. 536–581.
 - [28] J. M. MELENK AND S.A. SAUTER, *Convergence analysis for finite element discretizations of the Helmholtz equation with Dirichlet-to-Neumann boundary conditions*, Math. Comp., 79 (2010), pp. 1871–1914.
 - [29] ———, *Wavenumber explicit convergence analysis for Galerkin discretizations of the Helmholtz equation*, SIAM J. Numer. Anal., 49 (2011), pp. 1210–1243.
 - [30] A. NAGA AND Z. ZHANG, *A posteriori error estimates based on the polynomial preserving recovery*, SIAM J. Numer. Anal., 42 (2004), pp. 1780–1800.
 - [31] A.H. SCHATZ, *An observation concerning Ritz–Galerkin methods with indefinite bilinear forms*, Math. Comp., 28 (1974), pp. 959–962.
 - [32] J. WANG, *Asymptotic expansions and l^∞ -error estimates for mixed finite element methods for second order elliptic problems*, Numer. Math., 55 (1989), pp. 401–430.
 - [33] H. WU, *Pre-asymptotic error analysis of CIP-FEM and FEM for Helmholtz equation with high wave number. Part I: Linear version*, IMA J. Numer. Anal., 34 (2014), pp. 1266–1288.
 - [34] H. WU AND Z. ZHANG, *Can we have superconvergent gradient recovery under adaptive meshes?*, SIAM J. Numer. Anal., 45 (2007), pp. 1701–1722.
 - [35] J. XU AND Z. ZHANG, *Analysis of recovery type a posteriori error estimators for mildly structured grids*, Math. Comp., 73 (2003), pp. 1139–1152.
 - [36] N. YAN AND A. ZHOU, *Gradient recovery type a posteriori error estimates for finite element approximations on irregular meshes*, Comput. Methods Appl. Mech. Engrg., 190 (2001), pp. 4289–4299.
 - [37] Z. ZHANG, *Polynomial preserving gradient recovery and a posteriori estimate for bilinear element on irregular quadrilaterals*, Internat. J. Numer. Anal. Model., 1 (2004), pp. 1–24.
 - [38] ———, *Polynomial preserving recovery for anisotropic and irregular grids*, J. Comput. Math., 22 (2004), pp. 331–340.
 - [39] Z. ZHANG AND B. LI, *Analysis of a class of superconvergence patch recovery techniques for linear and bilinear finite elements*, Numer. Methods Partial Differential Equations, 15 (1999), pp. 151–167.
 - [40] Z. ZHANG AND A. NAGA, *A new finite element gradient recovery method: Superconvergence property*, SIAM J. Sci. Comput., 26 (2005), pp. 1192–1213.
 - [41] L. ZHU AND Y. DU, *Pre-asymptotic error analysis of hp-interior penalty discontinuous Galerkin methods for the Helmholtz equation with large wave number*, Comput. Math. Appl., 70 (2015), pp. 917–933.
 - [42] L. ZHU AND H. WU, *Pre-asymptotic error analysis of CIP-FEM and FEM for Helmholtz equation with high wave number. Part II: hp version*, SIAM J. Numer. Anal., 51 (2013), pp. 1828–1852.